Ecotoxicology and Environmental Safety 246 (2022) 114159

Contents lists available at ScienceDirect

Ecotoxicology and Environmental Safety

journal homepage: www.elsevier.com/locate/ecoenv

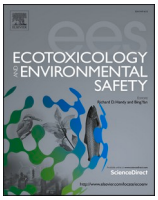

Phthalate plasticizer decreases the prion-like protein doppel essential for structural integrity and function of spermatozoa

Jae-Hyeon Lee [a,1], Seung Hyun Park [a,1], Chongsuk Ryou [b], Myung Chan Gye [a,*,2]

[a] Department of Life Science, Institute for Natural Sciences and Hanyang Institute of Bioscience and Biotechnology, Hanyang University, Seoul 04763, Republic of Korea
[b] College of Pharmacy and Institute of Pharmaceutical Science and Technology, Hanyang University, Ansan 15588, Republic of Korea

ARTICLE INFO

Keywords:
Di-n-butyl phthalate
Prnd
Spermatozoa
Sertoli cells
Testis
Mouse

ABSTRACT

Di-n-butyl phthalate (DBP), a well-known endocrine disruptor, causes male reproductive dysfunction. To understand the underlying mechanisms, we performed histological, endocrinological, and biochemical analyses and assessed the expression of genes involved in spermatogenesis and sperm function according to OECD test guideline 407. Following 28 days of administration of the lowest observed adverse effect level dose of DBP to mice, no significant changes in body weight, testis and epididymis weights and histology, serum testosterone level, or testicular daily sperm production were found. Nonetheless, the motility of the epididymal sperm of the DBP group was significantly decreased together with an increase in the incidence of bent tails and abnormal heads. In the testes of the DBP group, lipid peroxidation (LPO) level was significantly increased and testicular *Bcl-2* mRNA level was significantly decreased together with an increase in the *Bax/Bcl-2* mRNA ratio. In the testes of the DBP group, levels of *Prnd* mRNA and protein and *Pou4f1* mRNA, an activator of the *Prnd* promotor, were significantly decreased. Of note, prion-like protein doppel (PRND) was significantly decreased together with decreased PRND immunoreactivity in the head, midpiece, and tail of sperm. In the testes of the DBP group, levels of *Sox9, Sgp1*, and *Sgp2* mRNA, which are functional Sertoli cell markers, were significantly decreased. Level of *Amh* mRNA, a Sertoli cell immaturity marker, was significantly increased together with that of *Inha* mRNA, suggesting deregulation of the brain-gonadal axis. Together, our findings suggest that DBP at present dosage may potentiate LPO generation and Sertoli cell immaturity via downregulation of *Sox9* and disruption of the *Pou4f1-Prnd* gene network in post-meiotic germ cells without visible changes in spermatogenesis or testosterone level. This may result in structural and functional abnormalities in spermatozoa. Additionally, our findings suggest that assessment of the male reproductive toxicity of phthalate ester plasticizers based on conventional OECD test guidelines should be reconsidered.

1. Introduction

Phthalate plasticizers, which are well-known endocrine-disrupting chemicals, are widely used in the production of foods, consumer products, medical products, and industrial materials (Wang et al., 2021). Phthalates absorbed through dietary ingestion, inhalation, and skin absorption can cause many diseases in humans and wildlife (Wilson et al., 2001; Petrakis et al., 2017; Xu et al., 2022). Adult men are exposed to several phthalate esters, such as di-n-butyl phthalate (DBP), di-2-ethylhexyl phthalate, diethyl phthalate, and butyl benzyl phthalate (Wormuth et al., 2006). Several phthalate plasticizers and their metabolites have been detected in human urine and semen (Wormuth et al., 2006; Pant et al., 2008). In rats, DBP was detected in the testes of animals orally administrated corn oil only (Yin et al., 2016). DBP is a small-molecular weight chemical and not easily or spontaneously degradable, resulting in bio-enrichment (Wofford et al., 1981; Lyche, 2011). DBP has been implicated as the causative agent in various human diseases, including reproductive failure (Pant et al., 2008; Lyche et al., 2009; Park et al., 2015). DBP and mono-butyl phthalate, metabolites of DBP, are toxic to the male reproductive system of mammals (Lyche et al.,

* Correspondence to: Department of Life Science and Institute for Natural Sciences, Hanyang University, 222 Wangsimni-ro, Seongdong-gu, Seoul 04763, Republic of Korea.
E-mail address: mcgye@hanyang.ac.kr (M.C. Gye).
[1] These authors should be regarded as joint co-first authors.
[2] https://orcid.org/0000–0001-5682–3709

https://doi.org/10.1016/j.ecoenv.2022.114159
Received 30 June 2022; Received in revised form 2 October 2022; Accepted 4 October 2022
Available online 7 October 2022

2009). In humans, the DBP concentration in the semen of infertile men was significantly higher than those of fertile men (Pant et al., 2008). Male reproductive toxicity of DBP has been reported to vary by species, strain, age, toxicological endpoint, and dose–exposure period. In adult male rats, the lowest observed adverse effect level (LOAEL) of DBP on spermatogenesis, sperm function, and testosterone production has been reported to range between 200 and 250 mg/kg/day (Zhou et al., 2010; Aly et al., 2016). In neonatal mice, the LOAEL of DBP on testis development and anti-Müllerian hormone (AMH) production was reported to be 50 – 100 mg/kg/day (Moody et al., 2013), indicating that reproductive toxicity from neonatal exposure to DBP is much greater than that from adult exposure. In mammals, including humans, sperm dysfunction is the most common cause of male infertility and is associated with a variety of environmental pollutants, including endocrine disruptors, in addition to genetic makeup (Adewoyin et al., 2017). In humans, sperm morphology and sperm counts are both critical components of sperm fertility (Franken et al., 1989; WHO, 2010; Fujihara et al., 2012). To date, DBP has been shown to increase sperm abnormalities and spermatogenesis in mammals, but the mechanisms underlying the DBP-induced structural and functional abnormalities in sperm remain poorly understood.

Glycosylphosphatidylinositol (GPI)-anchored proteins on the membranes of secretory cells and endocytic organelles have diverse functions (Mayor and Riezman, 2004). Prion-like protein doppel (PRND/DPL) is a GPI-anchored membrane protein in the prion gene family (Allais-Bonnet and Pailhoux, 2014; Ciric and Rezaei, 2015). In mammalian testes, PRND is expressed in spermatids (Moore et al., 1999; Espenes et al., 2006; Allais-Bonnet et al., 2016). In mice, *Prnd* mRNA variants have been identified (https://www.st-va.ncbi.nlm.nih.gov/gene/26434), and non-, mono-, and di-glycosylated forms of PRND have been characterized (Silverman et al., 2000). Importantly, male mice lacking *Prnd* showed decreased sperm motility, sperm tail and head malformations, and decreased fertility (Behrens et al., 2002; Paisley et al., 2004).

To elucidate the mechanism by which DBP causes male reproductive toxicity, we evaluated changes in organ weights, lipid peroxidation, apoptotic gene expression, functional Sertoli cell markers, daily sperm production in the testes, and circulating testosterone level in adult male mice following 28 days of LOAEL dosing with DBP. As endpoints of DBP-induced reproductive toxicity to sperm structure and function, we examined changes in PRND and its transcriptional regulator in the testes and epididymal sperm; the morphology of the acrosome, sperm nuclei, and tail; and the motility of epididymal sperm. To the best of our knowledge, this is the first report that a phthalate ester plasticizers impairs the structural and functional integrity of spermatozoa via alteration of *Prnd* in male germ cells.

2. Materials and methods

2.1. Animals and drug treatment

Eight-week-old male C57BL/6 J mice were obtained from DAEHAN Biolink (Eumsung, Korea). Mice were housed in a pathogen-free authorized facility at Hanyang University, with the temperature maintained at 24 ± 2 °C and humidity at 50 ± 10% with a 12 h dark/light cycle. All experiments were carried out in accordance with the Institutional Animal Care and Use Committee (IACUC) guidelines of Hanyang University (IACUC No. 2019–0046A). Chemical administration was conducted according to OECD test guideline 407, which is an international standard of how to perform a repeat 28-day oral toxicity study in rodents (https://www.oecd-ilibrary.org/environment/test-no-407-repeated-dose-28-day-oral-toxicity-study-in-rodents_ 9789264070684-en; Xu et al., 2019). In detail, mice were divided into two groups, a control group and a DBP treatment group. After an adaptation period of one-week, mice received 200 mg/kg of DBP orally (D2270, Merck, Darmstadt, Germany), corresponding to the LOAEL dose for male reproductive toxicity in rodents for 28 days (Zhou et al., 2010; Aly et al., 2016). Corn oil (C8267, Merck) was used as the vehicle control. All mice were fasted for 12 h prior to euthanasia after 28 days of treatment. Body weights of all animals were measured on Day 0 before administration of the first dose and again 24 h after the final dose. Following ether anesthesia, blood was collected by cardiac puncture, and sera were isolated and stored at − 20 °C until measurement of testosterone concentration. Body organs were dissected, washed in PBS to remove blood, and weighed.

2.2. Hematoxylin & eosin (HE) staining

Testes were fixed with Bouin's solution (HT101128, Merck) overnight and then washed with 70% ethanol. Paraffin blocks were prepared using a standard protocol, and 5-μm-thick sections were attached to poly-L-lysine-coated slides. After deparaffination and hydration, samples were stained with hematoxylin for 2 min. After washing with PBS, slides were stained with eosin for 2 min, washed with PBS, dehydrated, cleared, and then mounted with Canada balsam (03984, Merck). Microscopic observation was conducted at x400 magnification, and slides were photographed using an FV300 microscope system (Olympus, Tokyo, Japan). Seminiferous tubule diameter and luminal area were analyzed using IMT iSolution Lite software (IMT iSolution Inc., Vancouver, BC, Canada) (Fig. S1).

2.3. Daily sperm production

Testicular daily sperm production (DSP) was examined according to Joyce et al. (1993). In brief, mouse testes were isolated and weighed, placed in 10 mL of PBS with 0.05% (v/v) Triton X-100, and then homogenized using a tissue tearor (985370–395, Biospec Products Inc., Bartlesville, OK, USA) at 15,000 rpm for 1 min. Homogenates were mixed with the same volume of trypan blue (0.04%) solution, and 10 μL was dropped onto a hemocytometer. The number of stage 14 – 16 spermatids was counted under a microscope (E200, Nikon, Tokyo, Japan). After counting five times per sample, averages were divided by testis weights to calculate the DSP. The numbers of spermatids per gram of testis were calculated and divided by 4.84 days for conversion to DSP.

2.4. Epididymal sperm collection and computer-assisted sperm analysis (CASA)

Epididymides were isolated and washed in PBS to eliminate blood, and cauda epididymides were dissected and placed in Tyrode's basal medium (TBM) and squeezed to release mature spermatozoa (García Herreros et al., 2005; Sotolongo et al., 2005). Motile spermatozoa were separated from epididymal tissue debris after incubation in a 5% CO_2 incubator at 37 °C for 20 min. After centrifugation at 500 x g for 5 min, sperm were resuspended in TBM and subjected to motility examination. Briefly, sperm samples were loaded into a pre-warmed Makler chamber, and sperm movement and the incidence of bent tails were examined using the iSperm CASA program (CNC Biotech, Suwon, Korea).

2.5. Examination of sperm acrosome, head, and tail morphology

Cauda epididymal sperm diluted in PBS were dropped onto slides coated with poly-L-lysine (P8920, Merck), dried, and then stored at −80 °C. Slides were fixed in a mixture of acetone and methanol (1:1) for 10 min and blocked with 3% bovine serum albumin (BSA, A9647, Merck) in PBS. Slides were stained with rhodamine-conjugated peanut agglutinin (PNA) (RL-1072, Vector, Burlingame, CA, USA) diluted 1:1000 in 1% BSA in PBS at room temperature (RT) for 1 h and then washed with PBS. After mounting with Prolong (P36931, Invitrogen, Carlsbad, CA, USA), the sperm acrosome and DAPI-stained head shape were observed using a fluorescence microscope system (DP71, Olympus) at x400 magnification. To assess tail morphology, microscopic observation was conducted at x400 magnification, and the tail was

photographed (E200, Nikon). Sperm morphology examination was based on at least 100 sperm per sample.

2.6. Lipid peroxidation (LPO) assay

To assess ROS-induced cellular damage in testes, LPO levels in testes were measured. After testes were weighed, the tunica albuginea was removed, placed in 20 volumes (w/v) of HPLC grade methanol (34860, Merck), homogenized using a tissue tearor (985370–395, Biospec Products Inc.) at 15,000 rpm for 1 min, and centrifuged at 1000 x g for 5 min. Thirty microliters of the supernatants and standards (30% H_2O_2, 23150s0350, Junsei, Tokyo, Japan) were pipetted into a 96-well plate (30096, SPL, Pocheon, Korea). After addition of 170 μL of substrate solution containing 90% methanol (HPLC grade), 100 μM xylenol orange (B0477, TCI, Tokyo, Japan), 25 mM sulfuric acid (258105, Merck), 250 μM iron(II) sulfate heptahydrate (F8633, Merck), and 4 mM 2,6-di-tert-butyl-4-methylphenol (B1378, Merck), plates were incubated at RT for 30 min. LPO levels were determined by absorbance at 570 nm using an iMark™ microplate reader (Bio-Rad, Hercules, CA, USA).

2.7. RNA isolation and real-time quantitative polymerase chain reaction (real-time qPCR)

Testicular *Amh, Bad, Bak1, Bax, Bcl-2, Bcl-w, Bcl-xl, Inha, Inhba, Inhbb, Lhr, Pou4f1, Prnd (v1–3, v4), Rhox5, Sgp1, Sgp2, Shbg,* and *Sox9* mRNA levels were evaluated by real-time PCR. Briefly, testes were homogenized in 10 volumes of Trizol reagent (79306, Qiagen, Hilden, Germany). Chloroform (C2432, Merck) was added to the samples, and mixtures were centrifuged at 14,000 rpm and 4 °C for 15 min. Supernatants were collected, the same volume of isopropanol (I9516, Merck) was added, and samples were incubated at 4 °C for 30 min and then centrifuged at 4 °C and 14,000 rpm for 10 min to precipitate the RNA. After two washes with 75% ethanol, RNA pellets were dissolved in nuclease-free distilled water, and the RNA concentration was adjusted to 500 ng/μL. After denaturation at 65 °C for 5 min, 5X RT Master Mix (ReverTra Ace® qPCR RT Kit, Toyobo, Osaka, Japan) was added, and then cDNA was synthesized by reverse transcription using an I-Cycler (T100, Bio-Rad) at 37 °C for 30 min, 50 °C for 5 min, and 98 °C for 5 min. To detect *Prnd* mRNA variants while avoiding amplification of *Prn* (*Prnd* and *Prnp* fused gene), mRNA specific primer sets targeting *Prnd v1–3* and *v4* mRNA were designed using https://www.ncbi.nlm.nih.gov/tools/primer-blast/, and their annealing temperatures were optimized (Table S1). *Rpl7* was used as the housekeeping gene. Primers, cDNA, and AccuPower® 2X GreenStar™ qPCR Master Mix (K-6253, Bioneer, Daejeon, Korea) were added to 0.2 mL PCR tubes, and real-time qPCR was conducted using a CFX Connect™ Real-time System (Bio-rad).

2.8. Western blotting

Testes and sperm were homogenized in lysis buffer containing 0.1% Triton X-100, 100X protease inhibitor (P3100–001, GenDEPOT, Katy, TX, USA), and 100X phosphatase inhibitor (P3200–001, GenDEPOT) in PBS, sonicated by a sonicator (HD2070, Bandelin, Berlin, Germany), and then centrifuged at 14,000 rpm and 4 °C for 20 min. Protein concentrations in the supernatants were determined using a BCA protein assay kit (23225, Thermo Fisher Scientific, Waltham, MA, USA). Samples were diluted with an appropriate stock solution of Laemmli sample buffer (Bio-Rad) and 5% DL-dithiothreitol solution (43816, Merck) and then boiled for 5 min. Following a brief spin-down, samples were subjected to SDS-PAGE using 10% and 12% running gels. After electro-transfer to a 0.2 μm nitrocellulose membrane (Whatman, Dassel, Germany) using a transblot (Bio-rad), blots were blocked with 7% skim milk (232100, BD Difco, Franklin Lakes, NJ, USA) in Tris-buffered saline (TBS) with 0.1% Tween 20 (P1379, Merck) (TBS-T) at RT for 1 h. Blots were probed with β-tubulin (1:10000, ab108342, Abcam, Cambridge, UK) and PRND (1:1000, ab23701, Abcam) as the primary antibodies and incubated at 4 °C overnight. After three washes for 20 min each with TBS-T, membranes were incubated with horseradish peroxidase–conjugated goat anti-rabbit IgG H&L (ab6721, Abcam) diluted in 5% skim milk/TBS-T for 1 h. After washing the samples three times for 20 min with TBS-T, chemiluminescence reagent (RPN2232, GE Healthcare Life Sciences, Uppsala, Sweden) was applied and blots were developed using Chemidoc reagents (Fusion SL, Vilber Lourmat, Eberhardzell, Germany).

2.9. Immunofluorescence of PRND in spermatozoa

Dry smeared sperm samples stored at − 80 °C were incubated at RT for 20 min and then fixed in a solution of acetone and methanol (1:1) for 10 min. Five percent donkey serum (ab7475, Abcam) was used as the blocking solution. Samples were probed with PRND (ab23701, Abcam) diluted 1:200 in blocking solution as the primary antibody and incubated at 4 °C overnight. Normal IgG (ab172730, Abcam) was used as a negative control. Alexa488-conjugated donkey anti-rabbit IgG (ab150073, Abcam) (1:200 dilution) was applied for 1 h as the secondary antibody. After a brief wash with PBS, rhodamine PNA solution (1:4,000 dilution) was applied for 1 h at RT to stain the acrosome. After washing the samples with PBS, we applied DAPI at RT for 1 h to stain the sperm nuclei. Sperm were observed using a fluorescence microscope system (DP71, Olympus). The immunoreactivity of PRND in the sperm head and tail was measured by assessing the fluorescence intensity of more than 29 spermatozoa using ImageJ software.

2.10. Serum testosterone assay

Blood was collected from the heart, and serum was isolated by centrifugation at 14,000 rpm for 10 min. Serum testosterone level was measured using a testosterone ELISA kit (DEV9911, de MediTech, Kiel, Germany).

2.11. Immunohistochemistry of PRND in testes

Testes were fixed in Bouin's solution (HT101128, Merck) overnight and then washed with 70% ethanol. Paraffin blocks prepared by the standard protocol were sectioned to a thickness of 5 μm and attached to poly-L-lysine-coated slides. After deparaffination and hydration, slides were quenched with 3.5% H_2O_2 in methanol and then blocked with 5% normal goat serum (S-1000, Vector) in PBS. Samples were then probed with anti-PRND rabbit polyclonal antibody (ab23701, Abcam) diluted 1:2000 in blocking solution and incubated at 4 ℃ overnight. Normal rabbit IgG (ab172730, Abcam) was used as a negative control. As the secondary antibody, goat anti-rabbit IgG (ab97051, Abcam) diluted 1:2000 was applied for 1 h at RT. After a wash in PBS, coloring development was initiated by adding 3,3′-diaminobenzidine (Vector) for 10 min. Slides were then stained with hematoxylin, dehydrated, cleared, and mounted with Canada balsam solution (03984, Merck). Samples were observed and photographed under a microscope (FV300, Olympus).

2.12. Statistical analysis

Statistical analyses were performed in SPSS (version 17.0; SPSS Inc, Chicago, IL) using unpaired, two-tailed Mann–Whitney *U* tests. Statistical significance was defined as *, $p < 0.05$, **, $p < 0.01$, and ***, $p < 0.001$.

3. Results

3.1. Changes in body and organ weights after DBP treatment

There were no significant differences in body, pituitary, testis, epididymis, ventral prostate, or seminal vesicles with coagulating gland weights between the control and DBP groups (Table S2).

3.2. Histological analysis of testes after DBP treatment

To evaluate the effects of DBP on spermatogenesis, testis histology was evaluated by HE staining. No atrophic changes were found in either the control or DBP group. No significant difference in seminiferous diameter or luminal area was found between the control and DBP groups (Fig. 1A, B and S1).

3.3. Changes in daily sperm production

To evaluate the effects on spermatogenesis, DSP was measured by counting spermatids. No significant differences in DSP were found between the control and DBP groups (Fig. 1C).

3.4. Changes in sperm motility after DBP treatment

Percentage of motile spermatozoa in DBP-treated mice was significantly lower than that in control mice (Fig. 2A).

3.5. Changes in sperm head abnormalities and bent tails after DBP treatment

PNA staining analysis of sperm revealed that the number of sperm with head, acrosomal, or nuclear deformities was significantly higher in the DBP group than in the control group (Fig. 2B, C and S2). Additionally, phase contrast image analysis of sperm tails revealed that the number of sperm with bent tails was significantly higher in the DBP group than in the control group (Fig. 2D).

3.6. Changes in LPO level in the testes after DBP treatment

Testicular LPO levels in the DBP group were significantly higher than those in the control group (Fig. 3A).

3.7. Changes in mRNA levels of pro- and anti-apoptotic genes in the testes

To investigate the effects of DBP on apoptosis, we examined mRNA levels of apoptotic genes by real-time qPCR. *Bax, Bad, Bak1, Bcl-xl,* and *Bcl-w* mRNA levels in the testes of DBP mice did not differ significantly from those in control mice, while the transcript level of *Bcl-2* was significantly decreased and the *Bax/Bcl-2* ratio significantly increased in DBP mice relative to control mice (Fig. 3B–H).

3.8. Changes in Prnd and Pou4f1 in the testes after DBP treatment

Prnd mRNA variants 1–3 but not variant 4 levels decreased significantly in the DBP group (Fig. 4A-B). To investigate changes in the *Prnd* gene activation network, we examined the expression of *Pou4f1*, a transcriptional activator of the *Prnd* promoter, in the testes. In the testes of the DBP group, *Pou4f1* mRNA level was significantly lower than in control mice (Fig. 4C). Multiple PRND protein bands corresponding to non-glycosylated, mono-glycosylated, and di-glycosylated forms were detected by western blotting, with total PRND level in the testes was significantly lower in the DBP group than the control group (Fig. 4D–E). Immunohistochemical analysis revealed strong PRND immunoreactivity in round spermatids and elongating/elongated spermatids in stages V–VI in the testes of control mice, which was visibly decreased in the testes of DBP-treated mice. No visible PRND immunoreactivity was observed when normal rabbit IgG was used rather than primary antibody (Fig. 4F).

3.9. Changes in sperm PRND protein level after DBP treatment

The di-glycosylated form of PRND was primarily expressed on the WB of cauda epididymal sperm, and total PRND level was significantly lower in the DBP-treated group than the control group. PRND was expressed in the acrosomes, midpieces, and tails of epididymal spermatozoa based on immunofluorescence labeling. Quantitative fluorescence image analysis revealed that the PRND immunoreactivity of sperm was significantly lower in DBP mice than control mice (Fig. 5).

3.10. Changes in the testicular mRNA levels of Sertoli cell functional markers and serum testosterone level after DBP treatment

To evaluate the effects of DBP on Sertoli cell functioning, we examined the expression of *Sox9, Sgp1, Sgp2, Rhox5, Shbg, Amh, Inha, Inhba*, and *Inhbb* mRNA as Sertoli cell markers. In DBP mice, testicular *Sox9, Sgp1*, and *Sgp2* mRNA levels were significantly lower than in control mice, whereas testicular *Amh and Inha* mRNA levels were significantly higher in DBP mice than control mice. Testicular *Rhox5, Shbg, Inhba*, and *Inhbb* mRNA levels did not differ significantly between the DBP and control mice (Fig. 6A-I). Serum testosterone level also showed no significant difference between control and DBP groups (Fig. 6J).

4. Discussion

4.1. DBP impairs the structural integrity and motility of spermatozoa

In mice, DBP and its metabolite mono-butyl phthalate (MBP) have been shown to decrease epididymal sperm count, increase sperm abnormalities, and impair testicular spermatogenic cells and Sertoli cells (Du et al., 2017). In the present study, no significant difference was observed in body weight between DBP-treated mice and control mice, suggesting that the LOAEL dose of DBP for male reproductive toxicity has no systemic toxicity in mice. Although 200 mg/kg of DBP has been

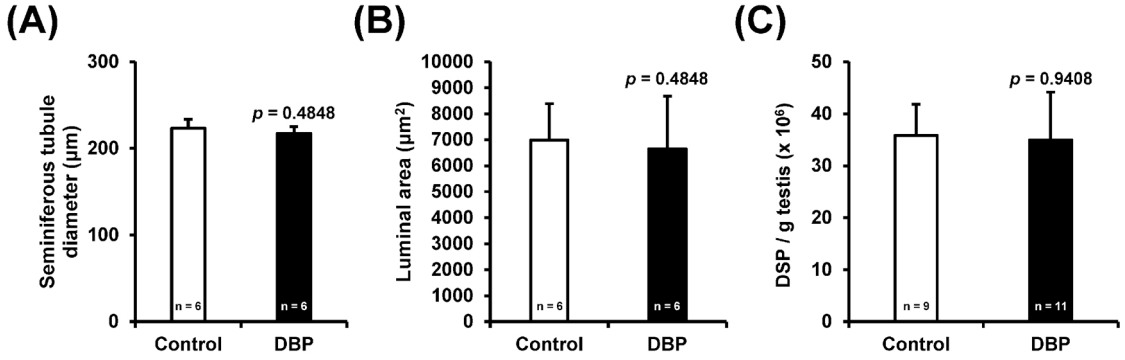

Fig. 1. Daily sperm production and histological analysis of the testes of adult male mice given 200 mg/kg of DBP for 28 days. (A) Change in the diameters of seminiferous tubules. Control (n = 6); DBP (n = 6). (B) Change in the luminal areas of seminiferous tubules. Control (n = 6); DBP (n = 6). (C) Daily sperm production in adult male mice. Control (n = 9); DBP (n = 11). Data are presented as means with standard deviations (error bars).

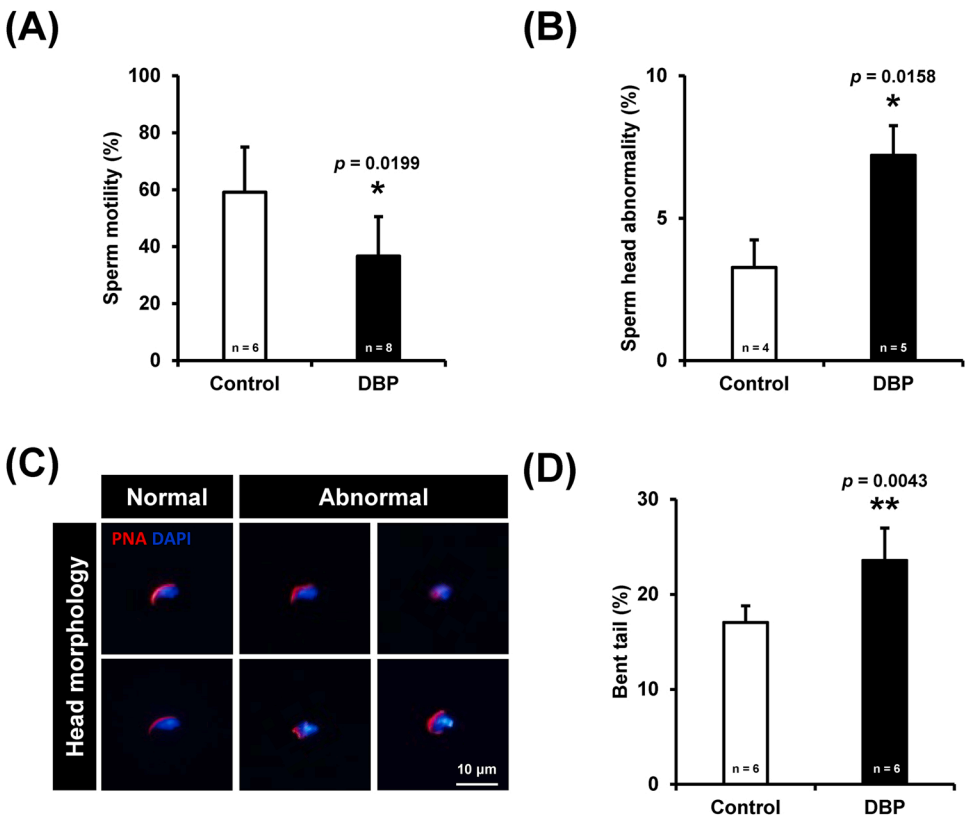

Fig. 2. Evaluation of the motility and morphology of the cauda epididymal sperm of male mice given 0 or 200 mg/kg of DBP for 28 days. (A) Changes in sperm motility ratio. Control (n = 6); DBP (n = 8). (B) Percentage of abnormal heads in cauda epididymal sperm. Control (n = 4); DBP (n = 5). (C) Classification of abnormal heads in cauda epididymal sperm. (D) Percentage of bent tails in cauda epididymal sperm. Control (n = 5); DBP (n = 6). Data are presented as means with standard deviations (error bars). * and ** indicate significant differences from the control group based on the two-tailed Mann–Whitney *U* test at $p < 0.05$ and $p < 0.01$, respectively.

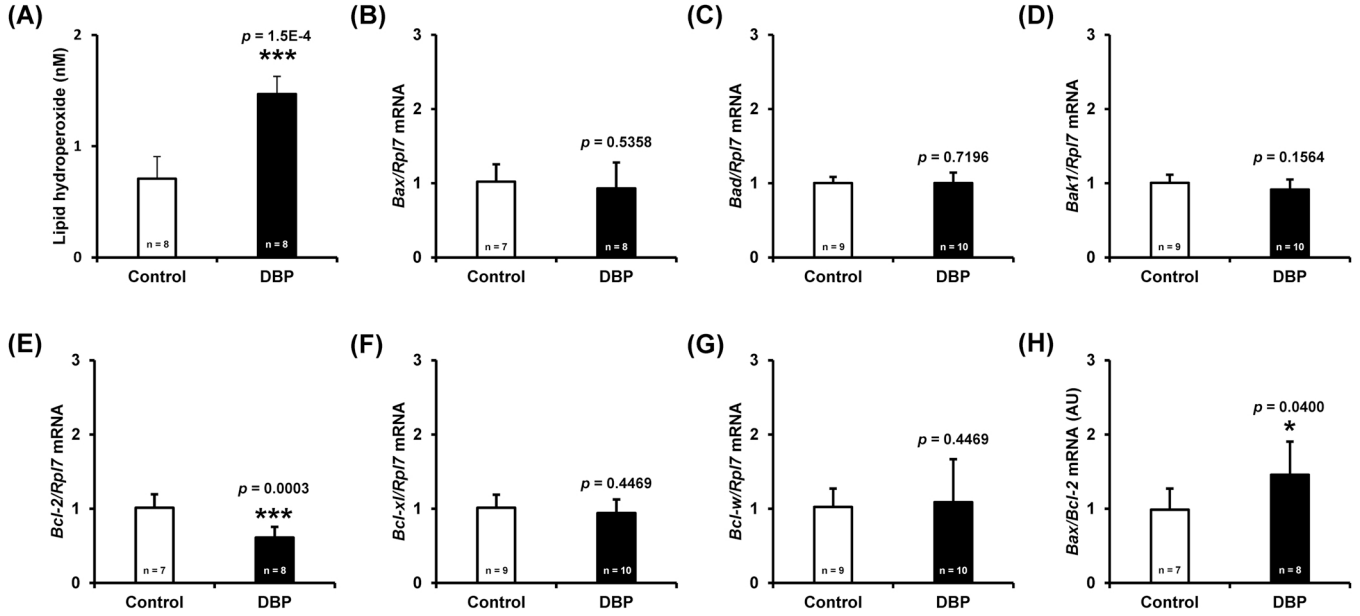

Fig. 3. Change in lipid peroxidation and apoptosis-associated gene mRNA levels in the testes of adult male mice given 0 or 200 mg/kg of DBP for 28 days. (A) Changes in LPO level in the testes after DBP treatment. (B - D) Real-time qPCR of the pro-apoptotic genes *Bax*, *Bad*, and *Bak1* in mouse testes. (E - G) Real-time qPCR of the anti-apoptotic genes *Bcl-2*, *Bcl-xl*, and *Bcl-w* in mouse testes. (H) *Bax/Bcl-2* ratio in mouse testes. Normalization was performed against the Ct values of *Rpl7* as an internal control. Control (n = 7 – 9); DBP (n = 8 – 10). Control (n = 8), DBP (n = 8). Data are presented as means with standard deviations (error bars). * and *** indicate significant difference from the control group based on two-tailed Mann–Whitney *U* test at $p < 0.05$ and $p < 0.001$, respectively.

reported to decrease testis weight in rats (Aly et al., 2016), paired testes weights, DSP, and the testis histology of mice given the LOAEL dose of DBP were not different from those of control mice. Given that spermatogonia are resistant to chemical insults including toxic alkylating agents such as busulfan (Choi et al., 2004), prolonged exposure to DBP may impair meiotic and/or post-meiotic germ cells rather than spermatogonia. In bulls, defective spermatozoa undergo phagocytosis in the epididymis (Sutovsky et al., 2001). This suggests that DBP may decrease epididymal sperm count without a change in testicular sperm count. Importantly, however, bent tails and acrosome dysgenesis were

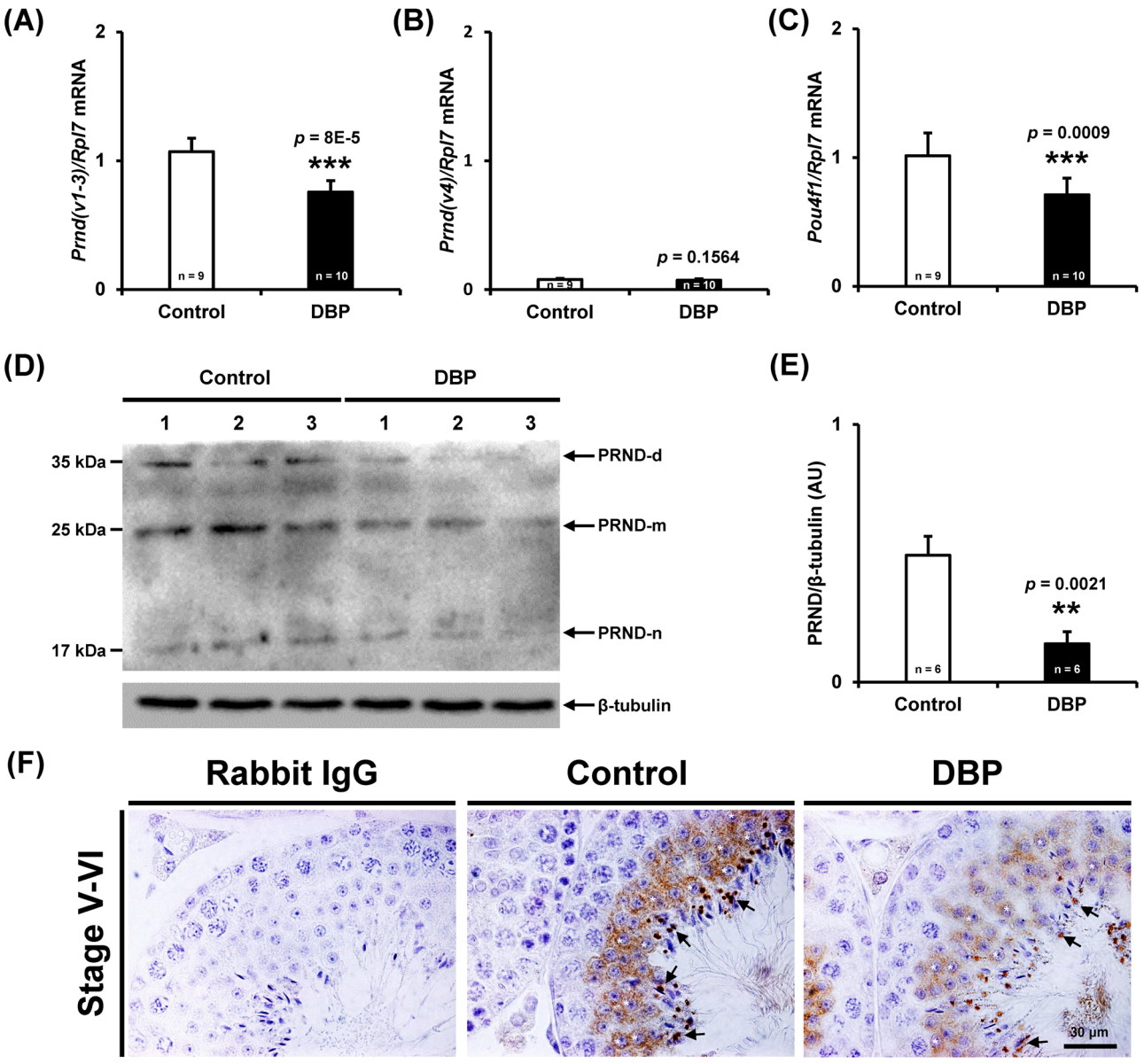

Fig. 4. Expression of *Prnd* and *Pou4f1* mRNA and PRND protein in the testes of adult male mice given 0 or 200 mg/kg of DBP for 28 days. (A and B) Real-time qPCR of *Prnd* variants 1–3 and variant 4 mRNA in mouse testes. Normalization was performed against the Ct value of *Rpl7* as an internal control. Control (n = 9); DBP (n = 10). (C) Real-time qPCR of *Pou4f1* mRNA in mouse testes. Normalization was performed against the Ct value of *Rpl7* as an internal control. Control (n = 9); DBP (n = 10). (D) Representative western blot of PRND in mouse testes. (E) Densitometry of PRND in mouse testes. Control (n = 6); DBP (n = 6). β-tubulin was used as the internal control. PRND-d, di-glycosylated PRND; PRND-m, mono-glycosylated PRND; PRND-n, non-glycosylated PRND. AU, arbitrary units. (F) Immunohistochemical imaging of PRND expression in testes. PRND-positive round spermatids and elongating/elongated spermatids are annotated by asterisks and arrows, respectively. Data are presented as means with standard deviations (error bars). ** and *** indicate significant differences from the control group based on two-tailed Mann–Whitney *U* tests at $p < 0.01$ and $p < 0.001$, respectively.

significantly increased and the motility of epididymal sperm was significantly decreased in DBP-treated mice relative to control mice. Similarly, in rats, DBP at 200 mg/kg/day increased sperm malformations and decreased sperm motility (Zhou et al., 2010; Aly et al., 2016). In mice, DBP at 200 mg/kg/day evoked no visible changes in anatomical and histological testis parameters but impaired the structural integrity and motility of sperm. Importantly, anatomical and histological examinations of the testes and DSP, major parameters of OECD test guideline 407, might be insufficient for evaluation of the potential male reproductive toxicity of endocrine disruptors such as phthalate ester plasticizers.

4.2. ROS is coupled with DBP-induced apoptotic damage in the testis

LPO, which is directly generated by the action of reactive oxygen species (ROS), is an important indicator of oxidative stress (Anand et al., 2014). In rats, increased testicular LPO is associated with decreased sperm count and motility and increased sperm morphological abnormalities (Kaya et al., 2019). In mice, MBP, a DBP metabolite, increased ROS in testis (Du et al., 2017). In DBP-treated mice, testicular LPO level was significantly higher than those in control mice. Similarly, rats given 200 mg/kg of DBP for 15 days showed elevated testicular LPO levels (Aly et al., 2016). Sperm plasma membranes have a high content of polyunsaturated fatty acids and are very sensitive to oxidative stress (Lenzi et al., 2000). Increased LPO levels could impair sperm structure, compromising sperm motility (Kao et al., 2008; Aitken et al., 2012).

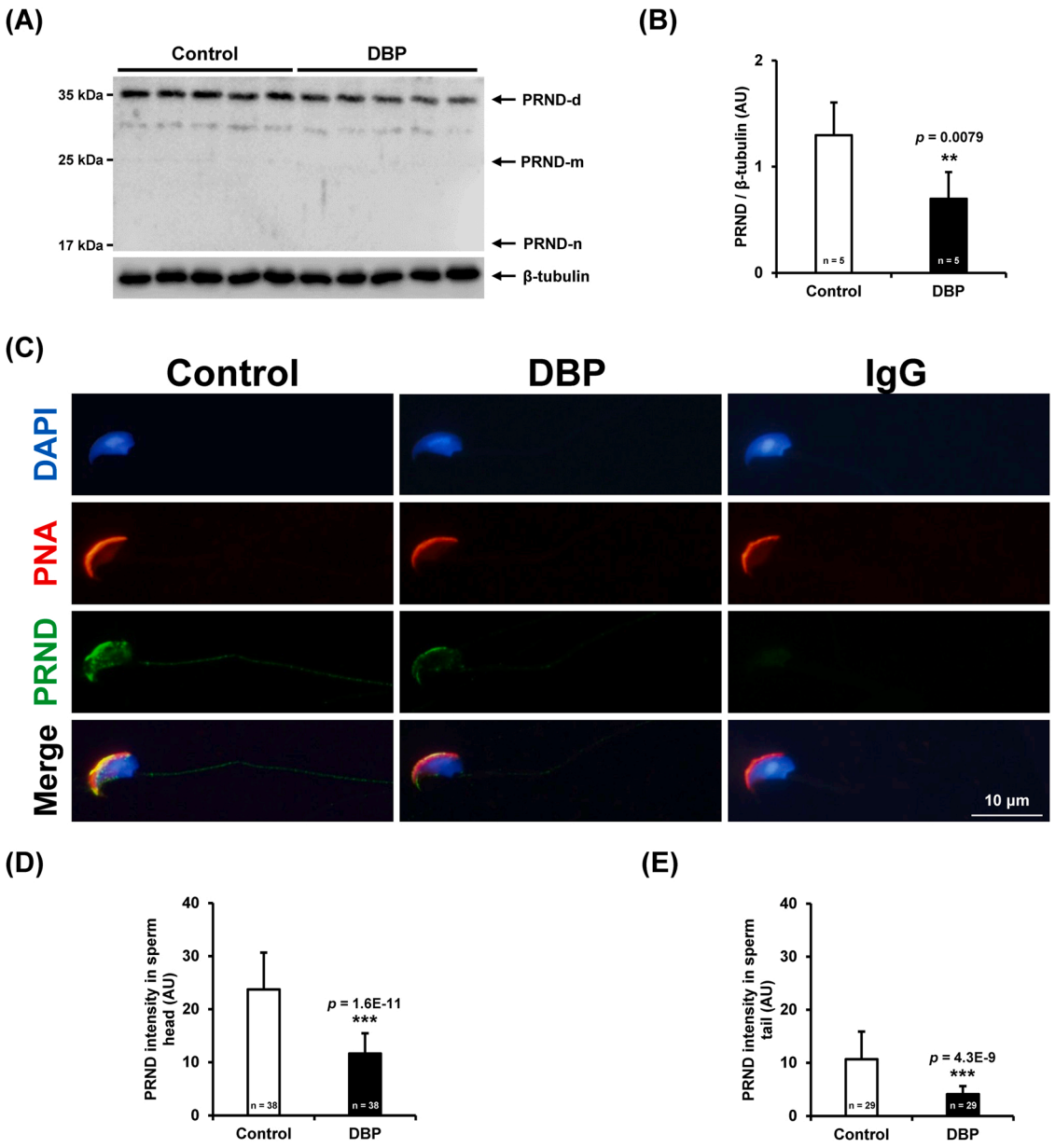

Fig. 5. Expression of PRND in the cauda epididymal sperm of adult male mice given 200 mg/kg of DBP for 28 days. (A and B) Western blot of PRND in mouse sperm. β-tubulin was analyzed as the internal control. Control (n = 5); DBP (n = 5). PRND-d, di-glycosylated PRND; PRND-m, mono-glycosylated PRND; PRND-n, non-glycosylated PRND. (C) Representative PRND immunofluorescence image of mouse cauda epididymal sperm. (D and E) PRND intensity in sperm heads and tails. Control (n = 29 – 38); DBP (n = 29 – 38). Data are presented as means with standard deviations (error bars). ** and *** indicate significant differences from the control group based on the two-tailed Mann–Whitney *U* test at $p < 0.01$ and $p < 0.001$, respectively.

Therefore, increased LPO in the testes might be the cause of both functional and structural sperm abnormalities. Although *Bax, Bad, Bak1, Bcl-xl,* and *Bcl-w* mRNA levels in the testes of DBP mice did not differ significantly from those in control mice, *Bcl-2* mRNA level was significantly decreased and the *Bax/Bcl-2* ratio was significantly increased in DBP-treated mice. This suggests that DBP may change the intratesticular environment to pro-apoptotic despite the absence of significant changes in DSP and testis weight. This also suggests that long-term DBP exposure could impair spermatogenesis by increasing cellular apoptosis.

4.3. PRND is coupled with DBP-induced structural and functional sperm abnormalities

Prnd mRNA and protein levels were significantly lower in the testes of the DBP group than those of the control group. PRND expression in spermatids was visibly decreased in the testes of DBP-treated mice, suggesting that DBP targets PRND in spermatids. POU4F1 (BRN-3A) is a transcription factor that binds and activates the *Prnd* promoter (Qin et al., 2013). Of note, testicular *Pou4f1* mRNA level in the DBP group was significantly lower than that in the control group, suggesting that DBP downregulates the *Pou4f1* – *Prnd* gene network. Sperm tail abnormalities are the primary cause of asthenozoospermia and are associated with decreased motility (Coutton et al., 2014). In *Prnd*-deficient male mice, sperm motility is decreased, and sperm tail and head malformations are observed at higher frequencies (Behrens et al., 2002). Of note, multiple PRND ranging in molecular weight from 17 to 35 kDa were detected in the WB of the testes, whereas the 35 kDa di-glycosylated form of PRND was primarily expressed in cauda epididymal sperm. This suggests that posttranslational modification of PRND by glycosylation increases during the late stages of spermatogenesis and epididymal

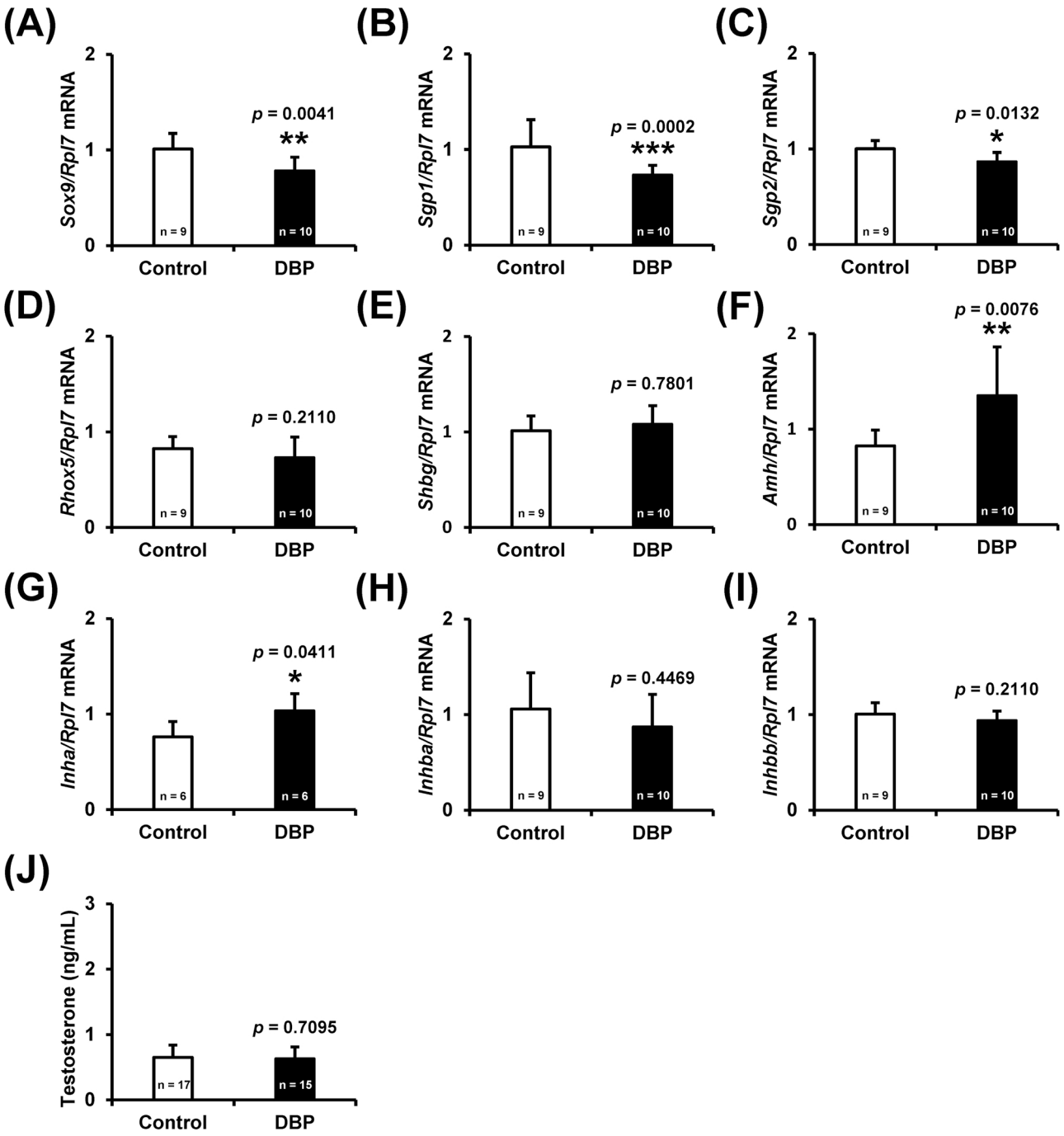

Fig. 6. Effects of DBP on the expression of Sertoli cell functional markers in the testes and circulating testosterone level of adult male mice given 200 mg/kg of DBP for 28 days. (A - I) Real-time qPCR analysis of *Sox9*, *Sgp1*, *Sgp2*, *Rhox5*, *Shbg*, *Amh*, *Inha*, *Inhba*, and *Inhbb* mRNA in mouse testes. Normalization was performed against the Ct value of *Rpl7* as an internal control. Control (n = 6–9); DBP (n = 6–10). (J) Changes in serum testosterone level of adult male mice given 200 mg/kg of DBP for 28 days. Control (n = 17); DBP (n = 15). Data are presented as means with SDs (error bars). *, **, and *** indicate significant differences from the control group based on two-tailed Mann–Whitney *U* tests at $p < 0.05$, $p < 0.01$, and $p < 0.001$, respectively.

maturation. In the DBP-treated group, the incidence of head deformity was significantly increased. Of note, total PRND level in the cauda epididymal sperm of the DBP group was significantly lower than that in the control group. PRND was found in the acrosome and sperm tail in both groups, similar to a previous study (Allais-Bonnet et al., 2016). In more detail, PRND immunoreactivity in the acrosomes and tails of epididymal sperm of the DBP group was significantly lower than that in the control group. PRND, a prion protein, is expressed in secretory and endocytic vesicles and interacts with the cytoskeleton; this protein is crucial for sperm fertility (Behrens et al., 2002; Paisley et al., 2004; Zafar et al., 2011; Allais-Bonnet and Pailhoux, 2014). Given that spermiogeneis in spermatids is contingent upon remodeling of the cytoskeleton, acrosome genesis, and discharge of cytoplasm, the DBP-mediated decrease in PRND could impair spermiogenesis to compromise sperm fertility, even in the absence of visible changes in DSP.

4.4. DBP increases Sertoli cell immaturity

Activin, which is suppressed by inhibin, stimulates proliferation and maturation of Sertoli cell (Ling et al., 1986; Stenvers and Findlay, 2010).

In mammals, inhibin inhibits FSH secretion via negative feedback (Makanji et al., 2014); in mice that overexpress *Inha*, testis size is decreased (McMullen et al., 2001). Given that DBP decreases circulating FSH level in male rats (Aly et al., 2016), the increased level of testicular *Inha* mRNA observed in DBP-treated mice suggests that DBP may disrupt the inhibin-FSH endocrine network. In DBP-treated mice, *Sox9, Sgp1*, and *Sgp2* mRNA levels were decreased together with an increase in the marker of immature Seroli cells, *Amh*. Similarly, in male mice, DBP increased both circulating AMH and testicular *Amh* mRNA levels (Moody et al., 2013). High concentration of AMH, a product of immature Sertoli cells, results in apoptosis of Sertoli cells and a decrease in testosterone production by Leydig cells (Holst, 2017; Rehman et al., 2017). These findings suggest that DBP at LOAEL dosing could induce the dysfunction or immaturity of Sertoli cells despite no visible histological changes in seminiferous tubules and circulating testosterone level. The adverse effects of DBP on testicular sperm function and structural integrity of spermatozoa could be due to insufficient support from Sertoli cells. In immature male mice, DBP has been shown to decrease testosterone level (Moody et al., 2013). We found that circulating testosterone level was not different significantly between control and DBP-treated mice. We attribute this to the insensitivity of Leydig cells to steroidogenesis in adult male mice treated with the LOAEL of DBP.

5. Conclusions

DBP may increase ROS damage and Sertoli cell dysfunction and downregulate the *Pou4f1-Prnd* network in germ cells, which could increase the incidence of bent tails and head abnormalities, impairing sperm motility even in the absence of visible changes in DSP and testosterone production. Assessment of male reproductive toxicity of phthalate ester plasticizers based on the conventional OECD test guideline should be reconsidered.

Funding

This work was supported by a grant (2020R1A6A1A03042854) from the Basic Science Research Program and a grant (2022R1A2C1007831) through the National Research Foundation of Republic of Korea (NRF).

CRediT authorship contribution statement

Jae-Hyeon Lee and Myung Chan Gye conceived and designed the experiments. Jae-Hyeon Lee and Seung Hyun Park performed the experiments. Jae-Hyeon Lee and Seung Hyun Park collected and analyzed the data. Chongsuk Ryou contributed reagents, materials, and analysis tools. Jae-Hyeon Lee, Myung Chan Gye, and Seung Hyun Park wrote the manuscript. All authors read and approved the final manuscript.

Declaration of Competing Interest

The authors declare that they have no known competing financial interests or personal relationships that could have appeared to influence the work reported in this paper.

Data availability

Data will be made available on request.

Appendix A. Supporting information

Supplementary data associated with this article can be found in the online version at doi:10.1016/j.ecoenv.2022.114159.

References

Adewoyin, M., Ibrahim, M., Roszaman, R., Isa, M.L.M., Alewi, N.A.M., Rafa, A.A.A., et al., 2017. Male infertility: The effect of natural antioxidants and phytocompounds on seminal oxidative stress. Diseases 5, 9.
Aitken, R.J., Whiting, S., De, Iuliis, G.N., McClymont, S., Mitchell, L.A., Baker, M.A., 2012. Electrophilic aldehydes generated by sperm metabolism activate mitochondrial reactive oxygen species generation and apoptosis by targeting succinate dehydrogenase. J. Biol. Chem. 287, 33048–33060.
Allais-Bonnet, A., Pailhoux, E., 2014. Role of the prion protein family in the gonads. Front. Cell. Dev. Biol. 2, 56.
Allais-Bonnet, A., Castille, J., Pannetier, M., Passet, B., Elzaïat, M., André, M., et al., 2016. A specific role for PRND in goat foetal Leydig cells is suggested by prion family gene expression during gonad development in goats and mice. FEBS Open Bio 6, 4–15.
Aly, H.A., Hassan, M.H., El-Beshbishy, H.A., Alahdal, A.M., Osman, A.M., 2016. Dibutyl phthalate induces oxidative stress and impairs spermatogenesis in adult rats. Toxicol. Ind. Health 32, 1467–1477.
Anand, A., Gupta, P.K., Prabhakar, S., Sharma, S., Thakur, K., 2014. Analysis of smoking and LPO in ALS. Neurochem. Int. 71, 47–55.
Behrens, A., Genoud, N., Naumann, H., Rülicke, T., Janett, F., Heppner, F.L., et al., 2002. Absence of the prion protein homologue Doppel causes male sterility. EMBO J. 21, 3652–3658.
Ciric, D., Rezaei, H., 2015. Biochemical insight into the prion protein family. Front. Cell. Dev. Biol. 3, 5.
Coutton, C., Escoffier, J., Martinez, G., Arnoult, C., Ray, P.F., 2014. Teratozoospermia: spotlight on the main genetic actors in the human. Hum. Reprod. Update 21, 455–485.
Du, J., Xiong, D., Zhang, Q., Li, X., Liu, X., You, H., et al., 2017. Mono-butyl phthalate-induced mouse testis injury is associated with oxidative stress and down-regulated expression of Sox9 and Dazl. J. Toxicol. Sci. 42, 319–328.
Espenes, A., Harbitz, I., Skogtvedt, S., Fuglestveit, R., Berg, K.A., Dick, G., et al., 2006. Dynamic expression of the prion-like protein Doppel in ovine testicular tissue. Int. J. Androl. 29, 400–408.
Franken, D.R., Oehninger, S., Johnson Burkman, L., Coddington, C.C., Kruger, T.F., Rosenwaks, Z., Acosta, A.A., Hodgen, G.D., 1989. The hemizona assay (HZA): A predictor of human sperm fertilizing potential in in vitro fertilization (IVF) treatment. J. Vitr. Fert. Embryo Transf. 6, 44–50.
Fujihara, Y., Satouh, Y., Inoue, N., Isotani, A., Ikawa, M., Okabe, M., 2012. SPACA1-deficient male mice are infertile with abnormally shaped sperm heads reminiscent of globozoospermia. Development 139, 3583–3589.
García Herreros, M., Aparicio, I.M., Núñez, I., García-Marín, L.J., Gil, M.C., Peña Vega, F. J., 2005. Boar sperm velocity and motility patterns under capacitating and non-capacitating incubation conditions. Theriogenology 63, 795–805.
Holst, B.S., 2017. Diagnostic possibilities from a serum sample—Clinical value of new methods within small animal reproduction, with focus on anti-Müllerian hormone. Reprod. Domest. Anim. 52, 303–309.
Joyce, K.L., Porcelli, J., Cooke, P.S., 1993. Neonatal goitrogen treatment increases adult testis size and sperm production in the mouse. J. Androl. 14, 448–455.
Kao, S.H., Chao, H.T., Chen, H.W., Hwang, T.I.S., Liao, T.L., Wei, Y.H., 2008. Increase of oxidative stress in human sperm with lower motility. Fertil. Steril. 89, 1183–1190.
Kaya, E., Ozer Kaya, S., Yilmaz, S., Ceribasi, A.O., Turk, G., 2019. Evaluation of ameliorating effect of lycopene against testicular toxicity due to diethylnitrosamine using biochemical, spermatological and histopathological data. Andrologia 51, e13274.
Lenzi, A., Gandini, L., Maresca, V., Rago, R., Sgrò, P., Dondero, F., et al., 2000. Fatty acid composition of spermatozoa and immature germ cells. Mol. Hum. Reprod. 6, 226–231.
Ling, N., Ying, S.Y., Ueno, N., Shimasaki, S., Esch, F., Hotta, M., 1986. Pituitary FSH is released by a heterodimer of the β-subunits from the two forms of inhibin. Nature 321, 779–782.
Lyche, J.L., 2011. Phthalates. Reprod. Dev. Toxicol. 2011 (48), 637–655.
Lyche, J.L., Gutleb, A.C., Bergman, A., Eriksen, G.S., Murk, A.J., Ropstad, E., et al., 2009. Reproductive and developmental toxicity of phthalates. J. Toxicol. Environ. Health B Crit. Rev. 12, 225–249.
Makanji, Y., Zhu, J., Mishra, R., Holmquist, C., Wong, W.P., Schwartz, N.B., et al., 2014. Inhibin at 90: from discovery to clinical application, a historical review. Endocr. Rev. 35, 747–794.
Mayor, S., Riezman, H., 2004. Sorting GPI-anchored proteins. Nat. Rev. Mol. Cell Biol. 5, 110–120.
McMullen, M.L., Cho, B.N., Yates, C.J., Mayo, K.E., 2001. Gonadal pathologies in transgenic mice expressing the rat inhibin α-subunit. Endocrinology 142, 5005–5014.
Moody, S., Goh, H., Bielanowicz, A., Rippon, P., Loveland, K.L., Itman, C., 2013. Prepubertal mouse testis growth and maturation and androgen production are acutely sensitive to di-n-butyl phthalate. Endocrinology 154, 3460–3475.
Moore, R.C., Lee, I.Y., Silverman, G.L., Harrison, P.M., Strome, R., Heinrich, C., et al., 1999. Ataxia in prion protein (PrP)-deficient mice is associated with upregulation of the novel PrP-like protein doppel. J. Mol. Biol. 292, 797–817.
Paisley, D., Banks, S., Selfridge, J., McLennan, N.F., Ritchie, A.M., McEwan, C., et al., 2004. Male infertility and DNA damage in Doppel knockout and prion protein/Doppel double-knockout mice. Am. J. Pathol. 164, 2279–2288.
Pant, N., Shukla, M., Kumar Patel, D., Shukla, Y., Mathur, N., Kumar Gupta, Y., et al., 2008. Correlation of phthalate exposures with semen quality. Toxicol. Appl. Pharmacol. 231, 112–116.

Park, S., Lee, J.M., Kim, J.W., Cheong, J.H., Yun, H.J., Hong, Y.C., et al., 2015. Association between phthalates and externalizing behaviors and cortical thickness in children with attention deficit hyperactivity disorder. Psychol. Med. 45, 1601–1602.
Petrakis, D., Vassilopoulou, L., Mamoulakis, C., Psycharakis, C., Anifantaki, A., Sifakis, S., et al., 2017. Endocrine disruptors leading to obesity and related diseases. Int. J. Environ. Res. Public Health 14, 1282.
Qin, K., Ding, T., Xiao, Y., Ma, W., Wang, Z., Gao, J., et al., 2013. Differential responses of neuronal and spermatogenic cells to the doppel cytotoxicity. PLoS One 8, e82130.
Rehman, Z.U., Worku, T., Davis, J.S., Talpur, H.S., Bhattarai, D., Kadariya, I., et al., 2017. Role and mechanism of AMH in the regulation of Sertoli cells in mice. J. Steroid Biochem. Mol. Biol. 174, 133–140.
Silverman, G.L., Qin, K., Moore, R.C., Yang, Y., Mastrangelo, P., Tremblay, P., et al., 2000. Doppel is an N-glycosylated, glycosylphosphatidylinositol-anchored protein. Expression in testis and ectopic production in the brains of Prnp(0/0) mice predisposed to Purkinje cell loss. J. Biol. Chem. 275, 26834–26841.
Sotolongo, B., Huang, T.T., Isenberger, E., Ward, W.S., 2005. An endogenous nuclease in hamster, mouse, and human spermatozoa cleaves DNA into loop-sized fragments. J. Androl. 26, 272–280.
Stenvers, K.L., Findlay, J.K., 2010. Inhibins: from reproductive hormones to tumor suppressors. Trends Endocrinol. Metab. 21, 174–180.
Sutovsky, P., Moreno, R., Ramalho-Santos, J., Dominko, T., Thompson, W.E., Schatten, G., 2001. A putative, ubiquitin-dependent mechanism for the recognition and elimination of defective spermatozoa in the mammalian epididymis. J. Cell Sci. 114, 1665–1675.
Wang, J., Zhang, X., Li, Y., Liu, Y., Tao, L., 2021. Exposure to Dibutyl Phthalate and Reproductive-Related Outcomes in Animal Models: Evidence From Rodents Study. Front. Physiol. 12, 684532.
Wilson, N.K., Chuang, J.C., Lyu, C., 2001. Levels of persistent organic pollutants in several child day care centers. J. Expo. Anal. Environ. Epidemiol. 11, 449–458.
Wofford, H.W., Wilsey, C.D., Neff, G.S., Giam, C.S., Neff, J.M., 1981. Bioaccumulation and metabolism of phthalate esters by oysters, brown shrimp, and sheepshead minnows. Ecotoxicol. Environ. Saf. 5, 202–210.
Wormuth, M., Scheringer, M., Vollenweider, M., Hungerbühler, K., 2006. What are the sources of exposure to eight frequently used phthalic acid esters in Europeans? Risk Anal. 26, 803–824.
Xu, Y., Park, S.H., Yoon, K.N., Park, S.J., Gye, M.C., 2019. Effects of citrate ester plasticizers and bis (2-ethylhexyl) phthalate in the OECD 28-day repeated-dose toxicity test (OECD TG 407). Environ. Res. 172, 675–683.
Xu, Y., Jang, J., Gye, M.C., 2022. The Xenopus laevis teratogenesis assay for developmental toxicity of phthalate plasticizers and alternatives. Environ. Pollut. 300, 118985.
Yin, L., Yan, L., He, B., Fang, Y., Liu, X., Duan, C., Yu, H., Peng, K., Wang, Q., Cheng, J., 2016. The toxic effects of a plasticizer, dibutyl phthalate, on rat testis. Int. J. Clin. Exp. Pathol. 9, 11246–11253.
Zafar, S., von Ahsen, N., Oellerich, M., Zerr, I., Schulz-Schaeffer, W.J., Armstrong, V.W., et al., 2011. Proteomics approach to identify the interacting partners of cellular prion protein and characterization of Rab7a interaction in neuronal cells. J. Proteome Res 10, 3123–3135.
Zhou, D., Wang, H., Zhang, J., Gao, X., Zhao, W., Zheng, Y., 2010. Di-n-butyl phthalate (DBP) exposure induces oxidative damage in testes of adult rats. Syst. Biol. Reprod. Med. 56, 413–419.